2007

Altered Parvalbumin-Positive Neuron Distribution in Basal Ganglia of Individuals with Tourette Syndrome

Paul S.A. Kalanithi
Yale University

Altered Parvalbumin-Positive Neuron Distribution In Basal Ganglia Of Individuals With Tourette Syndrome

A Thesis Submitted to the
Yale University School of Medicine
In Partial Fulfillment of the Requirements for the
Degree of Doctor of Medicine

By
Paul S. A. Kalanithi
2007

ALTERED PARVALBUMIN-POSITIVE NEURON DISTRIBUTION IN BASAL GANGLIA OF INDIVIDUALS WITH TOURETTE SYNDROME.

Paul Kalanithi[1], Wei Zheng[1], Yuko Kataoka[1], Marian DiFiglia[3,5]; Heidi Grantz[1]; Clifford B. Saper[4,5]; Michael L. Schwartz[2]; James F. Leckman[1]; Flora M. Vaccarino[1,2] [1]Child Study Center and [2]Department of Neurobiology, Yale University, New Haven, CT, [3]Department of Neurology and Program in Neuroscience, Massachusetts General Hospital, Charlestown, MA, [4]Beth Israel Deaconess Medical Center, Boston, MA, and [5]Harvard Medical School, Boston, MA, USA

The neuropathology of Tourette Syndrome (TS) is poorly characterized. This thesis provides the first quantitative stereologic immunohistochemical study of the basal ganglia in TS. TS is a childhood neuropsychiatric disorder characterized by motor and vocal tics. Previous imaging studies found alterations in caudate (Cd) and putamen (Pt) volumes. To investigate possible alterations in cell populations, postmortem basal ganglia tissue from individuals with TS and normal controls (NC) was analyzed using unbiased stereological techniques. A markedly higher (>160% of control) total neuron number and density was found in the internal segment of the globus pallidus (GPi) of TS ($p<0.025$). An increased number (>220% of control) and proportion of these GPi neurons were positive for the calcium-binding protein parvalbumin (PV) in the tissue from TS subjects ($p<0.025$). In contrast, a lower number (<60% of control) of neurons was observed in the external segment (GPe) ($p<0.025$). In addition, there was a lower density of PV-positive interneurons in both Cd (<50% of control) and Pt

(<65% of control) ($p>0.025$). The imbalance in striatal and GPi inhibitory neuron distribution suggests that the functional dynamics of cortico-striato-thalamic circuitry are fundamentally altered in severe, persistent TS.

– ACKNOWLEDGEMENTS –

I would like to thank my wife, Lucy, for her patience with my long nights and weekends in the lab, and the members of the Vaccarino Lab for welcoming me in to their space, and I would especially like to thank my mentors, Flora and Jim, for their exceeding generosity with their time, teaching, and encouragement, which has set the foundation for my future research career. To have one of them for a mentor was lucky; to have them both was a luxury.

We are grateful to Francine Benes, M.D., Ph.D., and the personnel at the HBTRC for their help in tissue preservation and storage, as well as for suggestions in tissue processing techniques. We are indebted to Brian Ciliax, Ph.D., and Neal Swerdlow, M.D., Ph.D., and to the other members of the TSA Scientific Advisory Board and Tissue Committee for organizing tissue collection and essential suggestions and encouragement.

Grant support was contributed by the following: NIH (P01 MH49351), the Tourette Syndrome Association, and the Yale School of Medicine.

– TABLE OF CONTENTS –

– INTRODUCTION –

A century ago, Ramon y Cajal described the state of central nervous system histology as "a number of unexplored continents and great stretches of unknown territory." One hundred years on, the neuropathology of neuropsychiatric diseases remains to be discovered. While 'purely' neurological diseases have a rich history of neuropathological investigation, 'purely' psychiatric diseases do not. Increasingly, the scientific consensus maintains that direct neurobiological investigation of psychiatric disease is necessary, though without neglecting important phenomenological work. TS, because it comprises both neurological and psychiatric components, is an ideal disease to begin this project. Like many neuropsychiatric diseases, neither the etiology nor the pathophysiology of Tourette Syndrome (TS) is well understood. A few models for the neural pathophysiology of TS exist, but these remain highly theoretical; while substantial clinical and imaging data exists for TS, the neuropathology of TS has rarely been investigated. To explore possible neuronal defects in TS, we undertook the first quantitative immunohistochemical study of TS.

I. Clinical Features of Tourette Syndrome

Tourette Syndrome (TS) is a childhood neuropsychiatric disorder characterized by persistent motor and vocal tics, affecting between 1 and 2% of children.[1] Motor tics usually begin around age 5, while vocal tics begin around age 12. Typically, tics occur in bouts, demonstrating a waxing and waning pattern of occurrence. Tic severity, for most TS sufferers, peaks in adolescence.[2] After this peak, tic symptoms variably decrease. However, in a distinct subset of patients, tics persist or reemerge in severe and

debilitating forms throughout adulthood. One prospective study of 46 children (mean age of 11) found that 22% had significant symptoms approximately 7.5 years later.[3] This was in accord with a previous survey showing that 28% of patients reported stable or worse symptoms 6 years later.[4] The cause of persistent adult TS remains unknown, but it has been shown to be related to caudate size[5], childhood tic severity[3], and fine-motor deficits[6].

While popular imagination has seized upon coprolalia as a distinguishing feature of TS, only a minority of patients exhibits such symptoms. Tics are repetitive, stereotyped motor movements that involve specific groups of muscles. Tics are characterized by their anatomic location, number, frequency, duration, complexity and intensity. Tics vary from simple (eye blinking or coughing) to complex (purposive appearing sequences, like brushing hair back or uttering phrases). Tics also vary from in their intensity, from subtle to forceful.[7] These factors are incorporated into rating scales used to assess and monitor TS severity.[8]

TS encompasses a wide spectrum of phenomena. Complex motor tics can sometimes be difficult to distinguish from other hyperkinetic movement disorders. However, TS is not purely a movement disorder. Tics are often preceded by sensory phenomena, akin to having an itch that can only be scratched by performing a tic. This pattern of urge and response shares a phenomenological similarity with OCD, and, interestingly, TS is strongly co-morbid with obsessive-compulsive behaviors and obsessive-compulsive disorder.[9] As such, TS is a quintessential neuropsychiatric disease, bridging movement disorders and anxiety disorders, and its study may shed light on a number of neuropsychiatric diseases.

II. The neurobiology of TS

Both genetic and environmental factors are thought to contribute to the development of TS, but the exact role of each has not yet been identified. Familial studies have documented vertical transmission, but no single major genetic vulnerability has been shown,* suggesting a genetic constellation for TS development.[11] Epigenetic events that increase the risk of developing tic disorder or TS are generally pre- and perinatal adverse events, including toxin exposure and complications of parturition. Most notably, perinatal hypoxic-ischemic events that damage the periventricular germinal matrix and adjacent deep regions of the brain increase rates of tic disorders.[12]

A considerable amount of data implicates the cortico-striato-thalamo-cortical (CSTC) circuits in TS pathophysiology, particularly basal ganglia (BG) abnormalities. The BG, a richly interconnected set of nuclei, are essential for the initiation and correct implementation of learned sequences of motor and cognitive segments that characterize purposive behavior. The BG appears to comprise several parallel circuits with distinct functions.[13, 14] For each circuit, the two major inputs into the basal ganglia, from the cerebral cortex and the intralaminar nuclei of the thalamus, enter into the striatum, which consists of the caudate (Cd) and putamen (Pt). Schemata of BG tracts vary with the number of tracts; one common division maintains three distinct pathways: the sensorimotor circuit, the associative circuit, and the limbic circuit. The sensorimotor

* Recently, mutations of the SLITTRK1 gene, implicated in neurite outgrowth, has shown an association with TS. Study of 174 unrelated TS subjects showed 3 with SLITTRK1 mutations, suggesting both the importance of SLITTRK1 as well as underlining polyfactorial contributions to the disease.(10. Abelson JF, Kwan KY, O'Roak BJ, et al. Sequence variants in SLITRK1 are associated with Tourette's syndrome. Science 2005; 310:317-20.)

CTSC circuit begins in the sensory and premotor areas and synapses in the Pt posterior to the anterior commissure; the associative CTSC circuit begins in the various association cortices in the frontal, temporal and parietal lobes and synapses in the anterior third of the Pt and throughout the Cd; finally, the limbic CTSC circuit begins in limbic cortex, including the amygdala and hippocampus, and synapses in the ventral striatum, including the nucleus accumbens. The rostral GP continues the associative circuit, the caudal GP the sensorimotor circuit, and the ventral GP the limbic.[13]

The predominant cell type of the striatum is the GABAergic medium spiny neuron (MSN). MSNs, which are the large majority of neurons in the striatum, project to the globus pallidus pars interna (GPi), either directly or indirectly via the subthalamic nucleus and the globus pallidus pars externa (GPe) (See Figure 1). These two pathways can be differentiated histologically: Substance P is contained within striatal terminals of the "direct pathway", while met-enkephalin is contained within terminals of the "indirect pathway". While this two pathway model is an extreme simplification, it has been useful in modeling other diseases of the BG, for example, Parkinson's.

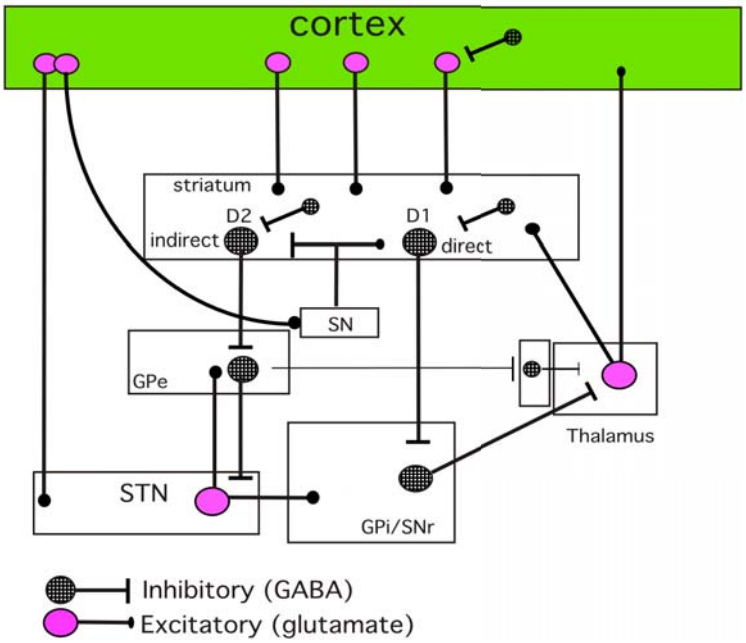

Figure 1. A schematic of the cortico-striato-thalamo-cortical loop.

Within the basal ganglia, two main pathways are thought to exist: the direct pathway, which runs from the striatum to the GPi /SNr to the thalamus, and the indirect pathway, which runs from the striatum to the GPe to the STN to the GPi/SNr. Within the striatum are PV+ interneurons, which appear to modulate striatal input and output. SN = substantia nigra; GPe = globus pallidus externa; GPi/SNr = globus pallidus interna/substantia nigra reticulata; STN = subthalamic nucleus.

MSNs form approximately 80% of the cells of the striatum, with interneurons accounting for the remainder.[15] There are four types of interneurons in the striatum: parvalbumin-positive (PV+), cholinergic (ACh), somatostatin/NPH-positive and calretinin-positive. These interneurons, except the ACh cells, are GABAergic. The functions of the calretinin-positive and NPH-positive cells are poorly understood, but the other cell types have been characterized. ACh interneurons receive input from thalamic nuclei, and synapse on the PV+ interneurons as well as the MSNs (See Figure 2). ACh cells are also called tonically-active neurons (TANs), and appear to play a role in regulating the response to reward-related stimuli.[15, 16] They are capable of both de- and

hyperpolarizing PV+ interneurons, and may be important in allowing local disinhibition of MSNs by curbing PV+ activity.[17]

The firing of cortical inputs drives activity in both medium spiny neurons (MSN)[18] and parvalbumin-positive (PV+) GABAergic interneurons.[19] Striatal PV+ interneurons are electrically coupled by gap junctions, forming a web of inhibitory synapses throughout the striatum.[20] The PV+ cells synapse on the somata of the MSNs, and electrophysiological studies demonstrate powerful inhibition and coordination of the activities of MSNs, likely altering the response to cortical inputs[21-24]. (See Figure 2)

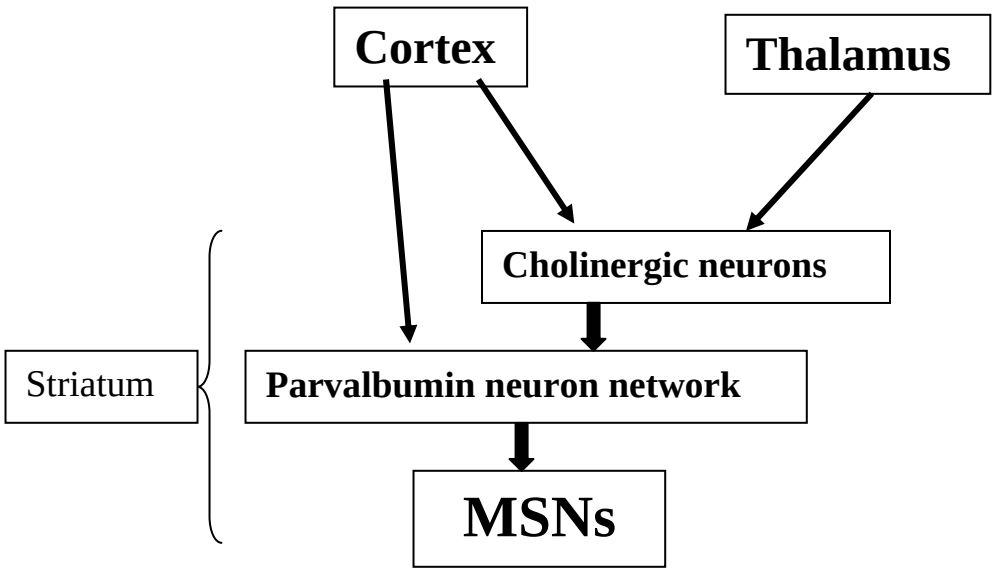

Figure 2. A schematic of inputs to the striatum and intrastriatal connections emphasizing parvalbumin neurons.

Parvalbumin positive neurons receive input from cortex and cholinergic neurons. Parvalbumin cells form an electrotonic network in the striatum. The parvalbumin network exhibits strong control over MSN firing, maintaining tonic inhibition of MSN activity. Local cholinergic input may inhibit a section of the PV+ network to allow MSN firing. MSNs = medium spiny neurons. While a great deal of evidence implicates the striatum in in TS pathology, our data provide evidence for a specific class of cells which may be defective in TS. Studies of these cells suggest that a defect in their function would be consistent with TS phenomenology. In particular, PV+ cells appear to integrate sensory and motor cortical inputs, regulate oscillation frequency, maintain the low rate of MSN baseline activity, and decrease desynchronous ('noise') firing from cortical inputs.

The GPi appears to provide the major output of the BG in humans.[25] The GP contains a high percentage of PV+ neurons: approximately 75% of GPi and 50% of GPe cells are positive for this calcium-binding protein.[26] However, unlike those in the striatum, PV+ cells in the GPi are projection neurons. The GPi inhibitory projections to the thalamus have a major influence on the firing rate and rhythmic activity of both ventrolateral and intralaminar thalamic nuclei,[27] which, then project back to the various origins in sensorimotor, associative or limbic cortex.

Each of these channels (sensorimotor, associative and limbic) forms a discrete pathway, and therefore, the possibility of specific phenomenological consequence when lesioned. Given the wide spectrum of phenomena in TS, it is not surprising that many major structures of the basal ganglia have been implicated in TS. Chemical and electrical stimulation of the Pt in both animals and humans can produce tic-like stereotypies.[28] Structural imaging studies have consistently shown small but significant decreases in Cd and Pt volumes in TS,[29] while functional imaging has shown decreased activity in the ventral striatum.[30-32] Treatment of TS pharmacologically involves dopamine and serotonin modulating agents, and as such alterations of these neurotransmitters might reasonably be thought to be involved in TS pathophysiology. While serotonin in TS has not been adequately studied, metabolic studies of dopamine terminals have suggested increased densities.[33] Additionally, levels of neuronal activity as measured by fMRI while patients are asked to actively suppress their tics are related in a complex manner to tic severity outside the magnet, such that neuronal activity in the head of the right Cd is inversely correlated with tic severity, whereas neuronal

activity in the GP and Pt is directly correlated with tic severity.[34] Intriguingly, therapeutic use of deep brain stimulation in TS generally targets the parafascicular and centromedian nuclei of the thalamus, which synapse on the ACh cells of the striatum, further implicating this circuitry in TS. [35-46]

These data, taken together, suggest strongly that the BG, particularly the striatum, are the primary location of TS pathology. Two general models of BG function and TS pathophysiology currently exist. The classical model, also known as the rate model, maintains that the primary function of excitation and inhibition is to alter the rate of firing of downstream neurons: inhibition acts as a 'brake' on neuronal activity. Neuronal activity, in this model, functions as an analog property.[47] An increase in activity of inhibitory neurons decreases the rate of firing of the neurons on which they synapse. This model, in which the indirect pathway is seen as opposed to the direct pathway, has offered a productive model of some movement disorders, where increases in direct pathway activity or decreases in indirect activity leads to hyperkinesis and, conversely, decreases in direct pathway activity or increases in indirect pathway activity lead to hypokinesis.

An alternative, emerging theory of BG function takes a state-dependant approach, classifying neuron activity according to varied frequencies: delta (< 2 Hz), theta (~2-7 Hz), alpha (~8-12 Hz), beta (~15-30 Hz) and gamma (30-80 Hz).[48-51] Synchrony at particular frequencies, and local areas of desynchrony, represent different states of functioning and information representation by, for example, modulating synaptic plasticity.[52, 53] In this model, the size of the neuronal population entrained is inversely related to oscillation frequency. PV+ interneurons are essential components in this

model. These cells, connected by gap junctions, are remarkable for their ability to fire at extremely high frequencies with little adaptation, narrow action potentials (APs) and rapid large-amplitude afterhyperpolarizations (AHPs)[23, 54, 55]. These properties are thought to be facilitated by PV, a calcium binding protein that may act as a calcium reserve in the cytoplasm of the cell. They synapse directly on the somata of MSNs, allowing strong control of MSN function[56]. Gap junctions, combined with the electrophysiologic properties of PV+ interneurons, allow regulation of electrophysiologic oscillations; additionally the PV+ neuron network, by receiving multiple cortical inputs, may act as a coincidence detector,[57] and through lateral inhibition of desynchronized cortical input, may increase signal fidelity and modulating through-put[57-61]. Evidence suggests these cells play this role not only in the BG, but in cortex as well.[61]

Defects in PV+ cells have the potential to form part of the pathophysiology of many neuropsychiatric diseases. In this paper, we investigate the possibility that defects in PV+ cells in the basal ganglia may form part of the neurohistological phenotype of TS.

– STATEMENT OF PURPOSE –

In an effort to better understand the cellular abnormalities that may be present in TS, we undertook the first quantitative postmortem study of the basal ganglia of individuals with TS as compared to age- and sex-matched normal controls (NCs), staining with cresyl violet, parvalbumin, met-enkephalin, and substance P.

Our hypothesis was as follows: TS may demonstrate histological abnormalities in the basal ganglia of the following kinds:

- a defect within the indirect pathway, in cell number, morphology or density, consistent with an impairment of inhibition of thalamocortical signaling
- an abnormality within the direct pathway, in cell number, morphology or density, consistent with hyperactivation of thalamocortical pathways
- an alteration in cell number, morphology or density of parvalbumin cells within the striatum, consistent with impaired cortical signal gating or oscillatory regulation
- an alteration in cell number, morphology or density of parvalbumin cells within the globus pallidus, consistent with impaired thalamic inhibition or altered oscillatory production

– METHODS –

Subjects.

A cohort of human brains obtained from the Harvard Brain Tissue Resource Center at McLean Hospital and the Yale Department of Critical Technologies was used in this study and included 5 normal controls (mean age, 60 ± 9.7) and 3 subjects with severe, persistent TS (mean age, 42 ± 11.9) (See Table 1). Normal control (NC) subjects were collected after routine autopsy at Yale University and Massachusetts General Hospital. The TS specimens were obtained following informed consent from the next-of-kin, and donated brain tissue was collected under the sponsorship of the Tourette Syndrome Association (TSA) tissue resource. This group of TS subjects was selected from a larger group of donated specimens (N=41). Reasons for exclusion included the presence of a neurological condition that might limit the interpretation of the findings, e.g., Alzheimer's disease, brain tumors, problematic agonal events (such as a prolonged interval on a respirator before death), or an excessive post mortem interval (N=17); an inability to locate the next-of-kin (N=5); the presence of a significant, severe comorbid psychiatric disorder, e.g., schizophrenia, bipolar disorder (N=8); or insufficient or improperly processed tissue (N=8). Tissue sections from one hemisphere were examined by routine neuropathological tests, and all TS or NC brains with any evidence of gross pathological changes or CNS cytological abnormalities, including cellular ischemic changes were excluded from analyses.

Each of the TS subjects was matched with one or more normal control subjects on the basis of age, postmortem interval, and, whenever possible, hemisphere (i.e., right vs left). All of subjects in this study were male.

Table 1. Subjects

Subject #	Stained with	Age, y	Sex	PMI	Cause of Death
YA99-7 (R)	CV	56	M	18	Peritonitis
Hcon (R)	CV, PV	47	M	21	Myocardial infarct
M96021 (L)	CV	65	M	8.5	Sepsis
Y98209 (R)	PV	59	M	20	COPD
Y98183 (R)	PV	73	M	12	Aortic dissection
Average		**60**	**M**	**16**	
TS Case #	**Stained with**	**Age**	**Sex**	**PMI**	**Mode of Death**
4187 (L, R)	CV, PV	54	M	11	Myocardial infarct
4454 (L, R)	CV, PV	37	M	27	Accidental overdose
4790 (L)	CV, PV	34	M	30	Myocardial infarct
Average		**42**	**M**	**23**	

Table 1. Basic subject data from which histological sections were obtained.

PMI= postmortem interval in hours. Differences in age and PMI were not significant by nonparametric statistics. Due to limitations of tissue supply, not all control brains could be evaluated for both total cell number by cresyl violet (CV) and PV+ cell density.

Psychiatric diagnoses were established using a retrospective review of medical records and an extensive family questionnaire that included the medical, psychiatric, and social history of the subjects. For the diagnosis of TS, Attention Deficit Hyperactivity Disorder (ADHD), obsessive-compulsive disorder, major depressive disorder, alcohol or drug dependence *DSM-IV* criteria were used. A best estimate procedure was used once all available data had been compiled (JFL, HG).[62] The TS diagnostic confidence index was also estimated.[63] All TS subjects had a "definite" *DSMIV* diagnosis of TS. They also had TS diagnostic confidence index Scores of >90, as well as a history of severe tic symptom severity, scoring 49-50 out of 50 points on the Yale Global Tic Severity Scale at the

"worst ever" point in their lives (See Table 2).[8] Two cases were associated with a positive family history for TS or chronic tics, and the third case with a history of perinatal hypoxia. One of the three TS subjects (case 4454) was not taking antipsychotic medications at the time of death. The other two subjects were on a variety of medications (Table 2). No subject in the NC group was receiving any psychotropic agents at the time of death.

Immunocytochemistry.

Intact half brains were stored in 10% formalin. The telencephalon and brainstem were cut coronally into 2.5 cm blocks, labeled A, B, C, D and E, from anterior to posterior. Blocks were rinsed in phosphate-buffered saline/0.1% NaN_3 (PBS/azide) and cryoprotected in 15% sucrose. Tissue was serially sectioned at 50 μm using a cryostat or a freezing microtome and 24 series of sections were collected.

Sections were rinsed 3 times in PBS, and endogenous peroxidase was quenched by incubation in 3% H_2O_2 for 30 min at room temperature. Sections were blocked in PBS containing 5% normal horse or goat serum and 0.1% Triton-X-100 (PBS-serum) for 30 min at room temperature and then incubated with the first antibody for 48 h at 4°C in PBS-serum. Primary antibodies were anti-parvalbumin (1:2500; Sigma, Saint Louis, MI); anti-substance P (1:1000; Immunostar, Hudson, WI) and anti-metenkephalin (1:1000; Immunostar). After 3 washes in PBS, sections were incubated with biotinylated secondary antibodies (Vectastain Elite kit, Vector, Burlingame, VT) in PBS-serum, and processed for immunoperoxidase staining according to manufacturer's instructions.

Table 2. Characteristics of the TS subjects			
Age	56	37	34
MOD	Myocardial infarct	Overdose of lithium, Clonazepam, OTC sedatives and stimulants	Probable myocardial infarct
DCI (0-100)	95	95	95
Age of onset	7.5	7.5	ND
YGTSS TIC WE (0-50)	49	50 WE at age 13 yrs	49 WE at age 30
Family history	Positive, multiple cases	Positive, a paternal grandfather	Negative
Developmental History*	No evidence of any difficulties	One febrile seizure at 18 mos; possible streptococcus infection	Perinatal hypoxia & prolonged labor
Problematic agonal history	Resuscitation efforts	None	None
Medications	Olanazapine 5 mg; Clonazepam 0.5 mg; Fluoxetine 30 mg	Prescription and OTC sedatives; Haloperidol, Pimozide, Clonidine and guanfacine in the past	Zisprasidone for 10 months prior to death; Clonazepam for 3 yrs; Pimozide for 10 yrs. Risperidone for 1 yr; Clonidine as a child

Table 2. Characteristics of TS subjects.
All cases ranked 95 in terms of certainty of TS diagnosis using the DCI (Diagnostic confidence index), a scale that measures the lifetime likelihood of having or of have ever had TS [63]. MOD= mode of death. YGTSS TIC WE= Worst ever Yale Global Tic Severity Scale [62]. ND =not determined. OTC= Over the counter

*Possibility that there may have been an injury to the brain early in development

Tissue from control and TS was processed concurrently and exposed to the substrate for exactly equal amounts of time.

Of the above, the cresyl violet staining, anti-metenkephalin and anti-substance P staining was performed by WZ and FV. WZ, FV and I performed the parvalbumin staining. WZ and FV performed most of the PV staining of blocks containing GP sections; of these I stained 2/9. I performed the PV staining of all (6/6) the sections containing Cd and Pt without GP (the anterior and posterior blocks).[†]

Stereological Analyses.

One series of sections, 1.2 mm apart, was stained with cresyl violet and subjected to unbiased stereological analysis using a Zeiss Axioskop 2 mot equipped with an automatic stage and coupled to a computer running StereoInvestigator and Neurolucida software. The Cd, Pt, GPe and GPi regions were drawn in each section in the series based on cytoarchitectonic landmarks. When applicable, the volume of these nuclei was estimated by planimetry, which is computed by adding up the cross-sectional areas of the nucleus of interest in each section and by multiplying this number by the section interval and by the average section thickness (measured at the time of counting).

Nuclear profiles were counted using the optical fractionator method with a 40X oil-immersion objective, by randomly placing a sampling grid over each contour. Sampling grids measured 1800 x 1800 μm for GPi and 1500 x 1500 μm for GPe. Tri-dimensional counting frames (180 x 180 x 15 μm for GPi and 130 x 130 x 15 μm for GPe) with 3 out of 6 exclusion borders[65, 66] were automatically placed by StereoInvestigator at each grid

[†] This applies to the data presented in this thesis and the resultant publication (64. Kalanithi PS, Zheng W, Kataoka Y, et al. Altered parvalbumin-positive neuron distribution in basal ganglia of individuals with Tourette syndrome. Proc Natl Acad Sci U S A 2005; 102:13307-12.). YK has continued this work; her additional data is discussed in footnotes.

intersection point. Approximately 412 frames were sampled in the GPe and 124 frames in the GPi. On average, 280 neurons per brain were counted in the GPe, and 81 in the GPi. Neurons and glia were separately counted in each frame, distinguished on the basis of their cytological appearance. The total number of cells per region was calculated by StereoInvestigator using the formula

$$N = \sum Q * t/h * 1/asf * 1/ssf$$

where $\sum Q$ was the total number of nuclei counted, t the mean section thickness, h the height of the optical dissector, asf is the area sampling fraction, and ssf is the section sampling fraction.[66] The density for each cell type was calculated by dividing the total number of cells by the total counting volume.

For the parvalbumin-stained sections, the protocol was identical to the above, except for the sizes of the sampling grids and counting frames. Sampling grid in the GP measured 1000 x 1000 μm, counting frames measured 130 x 130 x 15 μm. In the striatum the sampling grid measured 2500 x 2500 μm, and counting frame measured 700 x 500 x 15 μm. The counting frames were placed in the most superficial portion of the sections (1 μm from the surface), to avoid variability due to differential penetration of antibodies. Cell density within tissue was calculated by dividing the total number of cells by the total volume of tissue sampled. Approximately 356 frames were sampled in the Cd, 417 in the Pt, 368 frames in the GPe and 327 frames in the GPi. On average, a total of 244 cells per brain were counted in the Cd, 348 in the Pt, 172 in the GPe, and 244 in the GPi.

I performed the majority of the stereological counts, including counting almost all the PV immunostained sections presented here; of note, I recounted a significant

portion of the work performed by the other counters (WZ and YK), and the inter-person count variability was less than 3%. Additionally, I performed stereological counts and partial analysis of 12 blocks of insular cortex, which was aborted in order to focus purely on BG structures. Finally, using the Stereoinvestigator software and Excel, I performed all the quantitative analysis discussed in the Results and Discussion sections. Statistics were performed by MS.

– RESULTS –

I. Cresyl violet staining

CV staining is nonspecific, allowing assessment of neurons as well as glia, which can be distinguished by size. All brains from the TS cases showed an increase in both density and total neuron number in the GPi as compared to NC (See Table 3). These changes were remarkably consistent in our sample, such that the differences in total neuron number in the GPe and GPi between NC and TS were statistically significant despite the small number of patients.

No change in size or shape of the neuronal cell bodies was noted. The total number, density and morphology of glial cells did not differ among TS or control brains in either the GPe or GPi. No differences in the volume of the GPe or the GPi were detected among the subjects (See Table 3).

Table 3. Differences in total cell number in the Basal Ganglia of NC and TS

		Volume (mm^3)	Tot. Neuron No. (x 10^3)	Neuron density (10^3 cells/mm^3)	Total glial No. (x10^6)	Glial density (10^3 cells/mm^3)
GPe	NC	491.4 ± 41.1	1695 ± 304	3.41 ± 0.36	177 ± 21.4	372 ± 74.6
	TS	442.4 ± 10.5	910 ± 105*****	2.05 ± 0.20*****	158 ± 6.2	358 ± 17.6
GPi	NC	223.2 ± 32.8	540 ± 49	2.54 ± 0.46	63.5 ± 2.1	297 ± 42.5
	TS	230.0 ± 25.7	905 ± 108 *****	4.00 ± 0.54	72.4 ± 9.1	319 ± 39.4

Table 3. Morphometric analysis of globus pallidus subregions after cresyl violet staining in NC and TS patients. Values represent group means ± SEM. The volume, total cell number and density was assessed in serial sections by stereological analyses using StereoInvestigator, as described in the text.

* TS versus NC statistically different; $p<0.025$, Mann-Whitney U test.

Table 4	**Density (cells x 1000/ mm³ ± SEM)**		
	NC	TS	TS/NC (%)
Cd (head)	41.1 ± 6.7	40.2 ± 2.6	-2.2
Cd (body)	57.1 ± 4.4	41.3 ± 2.6*	-27.6
Pt	42.5 ± 4.0	36.0 ± 2.6	-15.0

Table 4. Cell density of striatal subregions after cresyl violet staining in NC and TS subjects. Values represent group means ± SEM. Cell density includes measurements of MSNs, glia and interneurons. The volume, total cell number and density was assessed in serial sections by stereological analyses using StereoInvestigator, as described in the text.

* TS versus NC statistically different; $p<0.025$, Mann-Whitney U test.

Cresyl violet staining of the striatum revealed a general decrease in cells in the body of the Cd: TS subjects appeared to have 28% fewer cells. In the Cd head and the Pt, no significant difference in cell density was detected (See Table 4). No morphological differences were noted between the cells of TS and NC subjects.

II. Parvalbumin staining

We immunostained sections for parvalbumin (PV), which is normally expressed by the majority of GP cells and assessed the density of these cells in various regions of the basal ganglia by unbiased sampling methods. The density of PV+ cells was higher by 122% in the GPi of the subjects with TS as compared to NC. In contrast, the brains from TS subjects exhibited a lower density of PV+ neurons in all other basal ganglia regions assessed. This difference was strongest in the Cd (51% lower), smaller in the Pt (37%), and the smallest in the GPe (23%) (See Figure 3).

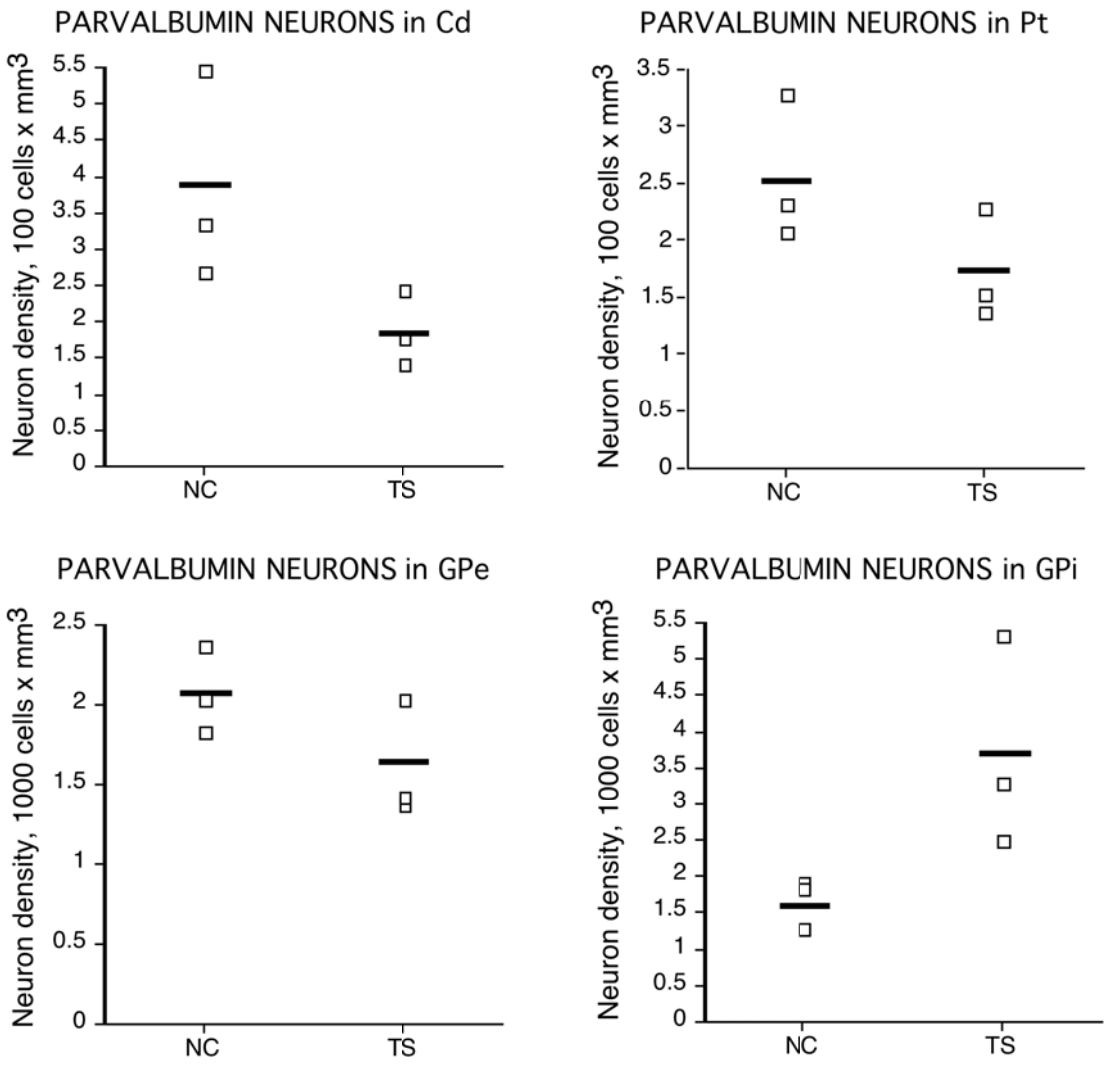

Figure 3. *Unbiased estimates of PV cell density in three TS and three NC brains.*

Each small square represents a single subject. Cd, Caudate; Pt, Putamen; C, GPe, Globus Pallidus Pars externa; D, GPi, Globus Pallidus Pars interna. Differences in PV neuronal density in the Cd, Pt, and GPi of TS patients were statistically significant ($p<0.025$, Mann Whitney U test).

PV+ cells in both pallidal regions are large, multipolar projection neurons. This morphology did not appear to differ in the brains of TS subjects (See Figure 4). In the striatum, in contrast, PV+ cells are much smaller and display an extensive dendritic/axonal tree. Again, no apparent difference in PV cell morphology was present in the Cd and Pt of brains of TS cases as compared to NCs (see Figures 5, 6). The density of PV immunoreactivity in the neuropil (presumably reflecting the dendrites and axons of these cells) was clearly decreased in the Cd and Pt of TS cases as compared to corresponding regions of NCs (See Figure 5).

To estimate the total number of PV+ cells, we multiplied the PV+ cell density in the GPi and GPe of each subject by the corresponding volumes (See Table 4). The results suggest that the number of PV+ neurons was 30.8% smaller in the GPe of patients with TS, while it was 129% larger in the GPi of patients with TS in comparison to NC. These changes are virtually identical to those noted for PV+ neuron density in these regions, as total volumes were not significantly different between the groups. For the Pt and the Cd, we could not obtain total volumes by stereological analyses with the available tissue. To have an estimate of total number of PV+ neurons in these regions for comparison to the GP data, we used an extensive neuroimaging dataset of 130 NCs and 154 TS subjects[29] and used their average Cd and Pt volumes after correcting for shrinkage due to tissue processing (see Table 4 legend).

Parvalbumin stained sections of the GPi

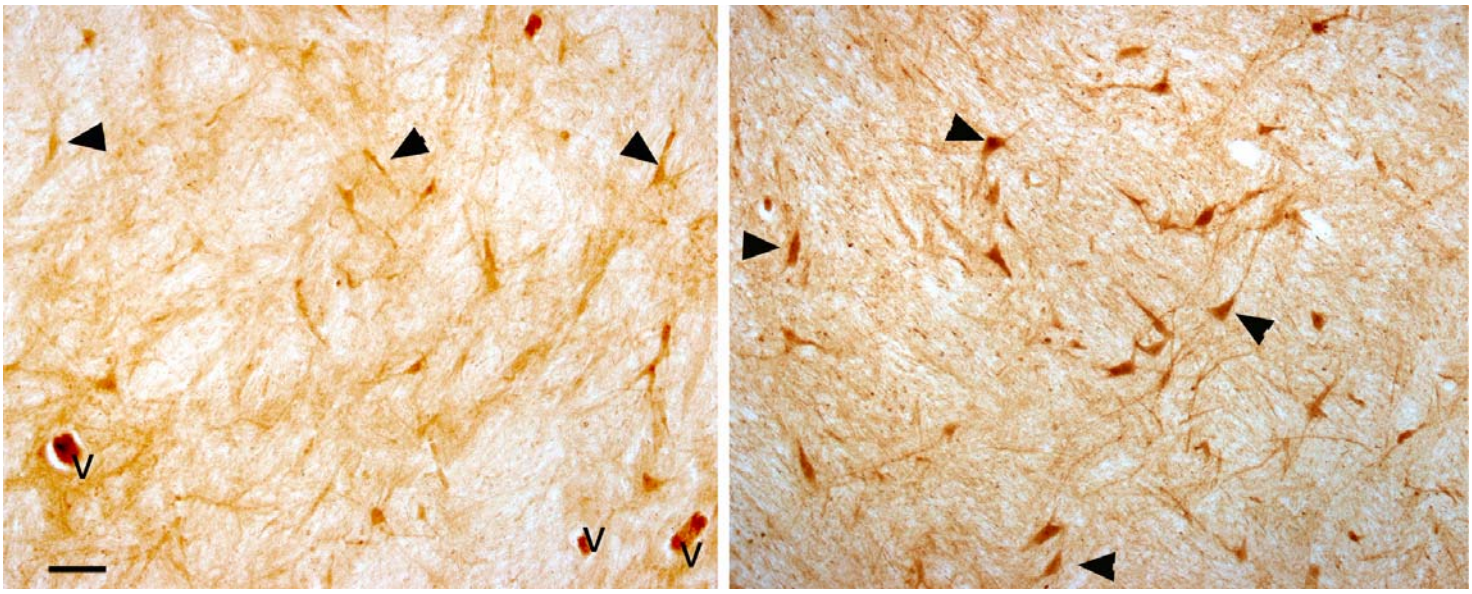

A. Control tissue

B. TS brain

Cresyl violet stained sections of the GPi

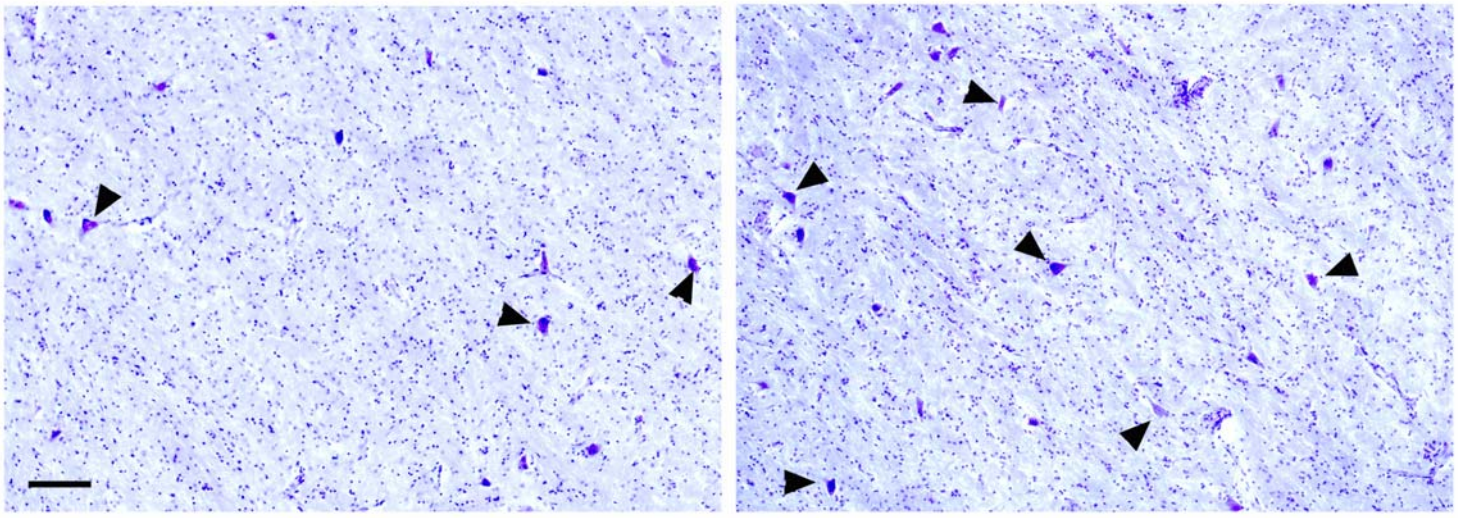

C. Control tissue

D. TS brain

Figure 4. Sections of GPi.
Increase in number of PV-containing neurons in the GPi of TS patients. A,B: PV immunostaining; C,D: cresyl violet staining. Representative sections from the GPi of NC (A,C) and TS (B,D) are shown. The morphology of the GPi neurons appears the same between TS and control. V=vein. Arrows indicate projection neurons. Scale bar, 100 μm.

Parvalbumin staining of the Cd

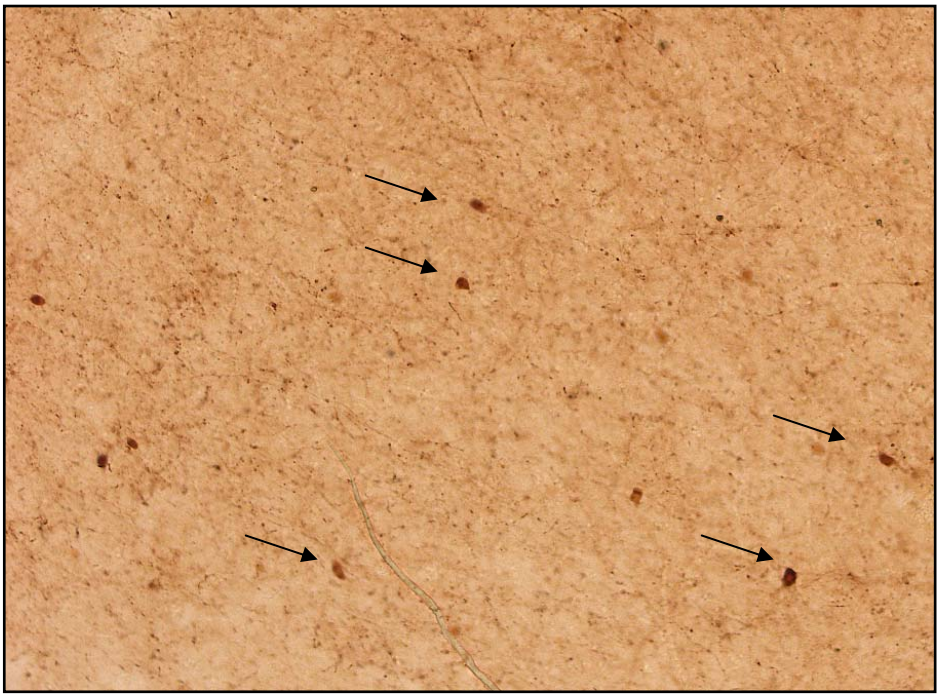

A. Normal control

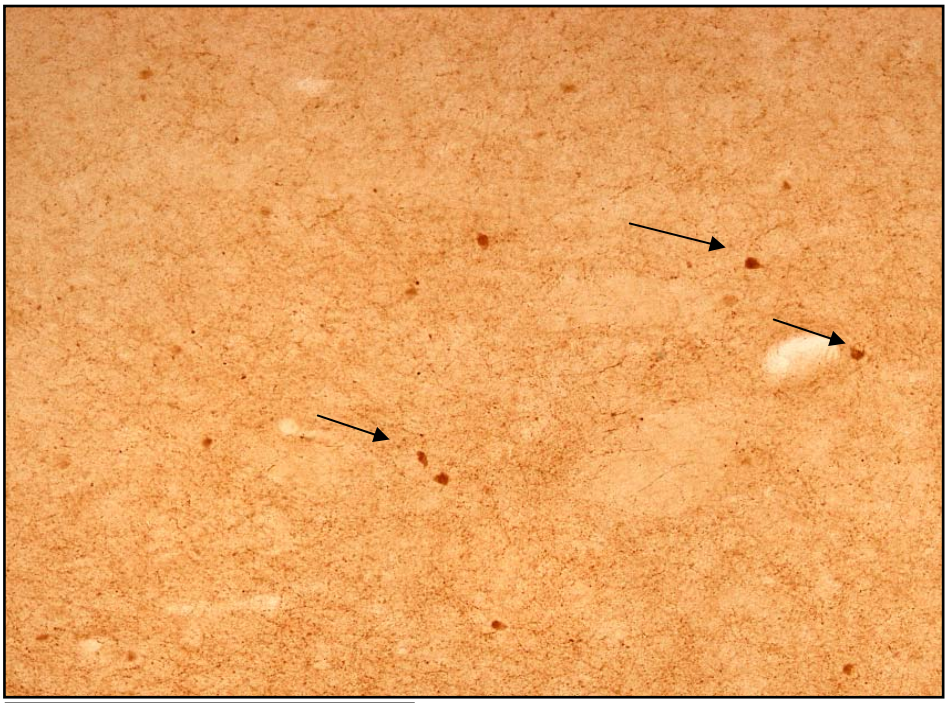

B. TS

Figure 5. Parvalbumin stained sections of the caudate.
Arrows indicate PV+ fast-spiking GABAergic interneurons.

A. Normal control

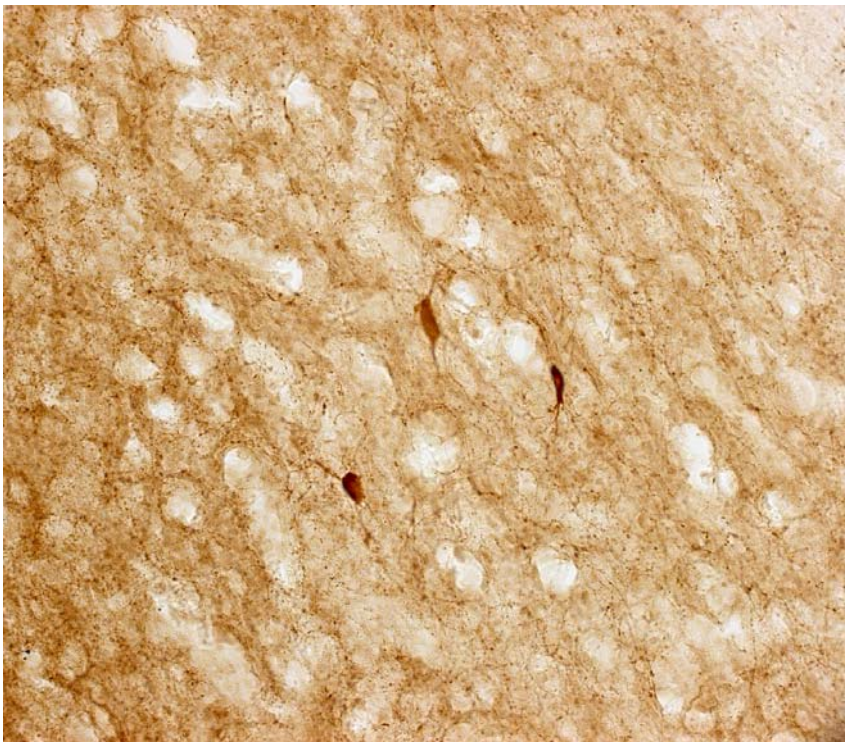

B. TS

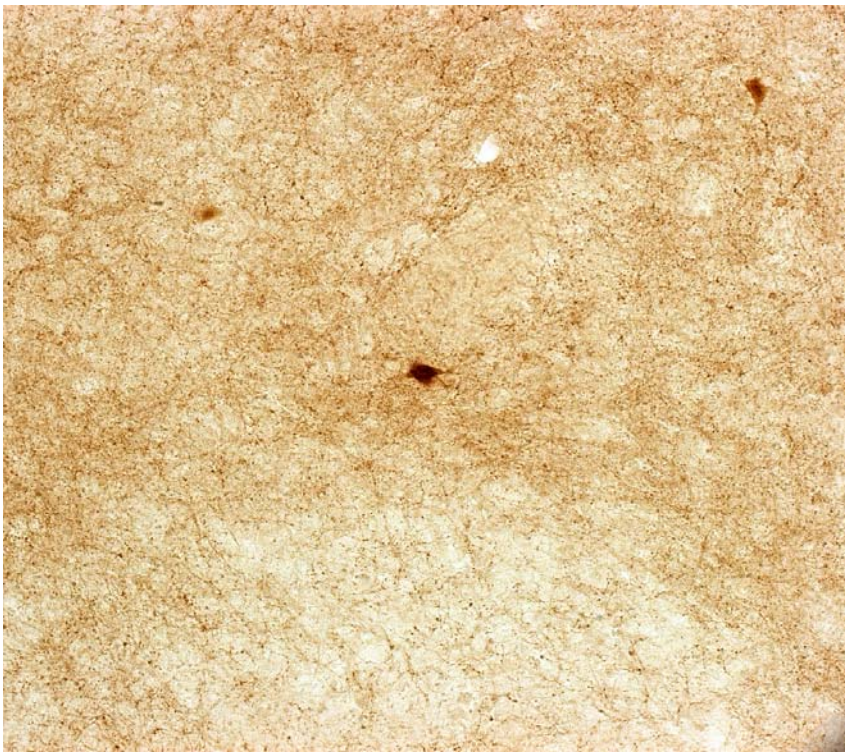

Figure 6. Parvalbumin staining in the Putamen.
The morphology of the cells does not appear to differ between TS and control.

Table 5. Number of parvalbumin neurons in TS			
	Total PV cell number		
	NC	TS	Difference (%)
Cd	572,000	266,000	-53.5
Pt	548,000	333,000	-39.3
GPe	1,020,000	707,000	-30.8
GPi	369,000	846,000	+129
Total	2,509,000	2,152,000	-14.2

Table 5. **Calculated number of PV neurons in TS**. To derive total cells, we multiplied our average PV density for the average volume obtained after tissue processing (Table 3). For the Cd and Pt, we used published in vivo volumetric data[29], which were first corrected according to a shrinkage factor of 0.40%. The shrinkage factor was obtained by dividing our GP volume (the sum of GPe and GPi calculated by stereological analyses after tissue processing) to that of Peterson et al[29]. Virtually identical volumes were obtained for the combined GP (GPe and GPi) applying the neuroimaging dataset after shrinkage correction and stereology (715 and 672 for NC and TS subjects, respectively, using stereology; and 712 and 674 NC and TS subjects, respectively, using neuroimaging after correction).

The results, reported in Table 5, suggest that the number of PV+ neurons was 53.5% and 39.3% smaller in the Cd and Pt, respectively, of patients with TS in comparison to NC. These changes in total PV+ cell number between NC and TS individuals are again similar to those reported in Figure 1 for PV+ cell density. Interestingly, the total number of PV+ neurons in the basal ganglia was decreased in TS by only 14.0% ($p > 0.025$, not statistically significant), suggesting that this group of TS patients differ with respect to the NC with respect to the distribution of PV neurons, and indicate the possibility that the overall number of PV neurons in the basal ganglia remains unchanged. (See Figure 8, in the Discussion.) However, given the small sample size, no firm conclusion regarding total numbers of PV cells can be drawn.

By subtracting the total parvalbumin neuron number from the total neuron number, we estimated changes in parvalbumin-negative neurons. However, we did directly assess PV-negative cells; thus these numbers are only estimates. The GPi of cases with TS appeared to have substantially fewer parvalbumin-negative cells: the GPi of control brains had 1.7 x 10^5 parvalbumin-negative neurons, while the GPi from subjects with TS had less than half that number, 7.0 x 10^4. In the GPe of the subjects with TS there were also fewer parvalbumin-negative neurons, 2.0 x 10^5 compared to 6.7 x 10^5. The differences were roughly similar, of 59% in the GPi and 69% in the GPe.

A post-hoc analysis of this data was performed to examine whether the changes in density varied by location within the BG subregions examined. Following prior studies of PV distribution,[67] the Pt, GPe and GPi were separated into rostral and caudal segments at the anterior commissure.

	rGPi	cGPi	rGPe	cGPe	rPt	cPt
Control (x1000/mm$^{3)}$	21.6	15.2	23.5	17.2	2.79	2.59
TS (x1000/mm$^{3)}$	37.4	34.8	14.1	17.3	2.41	1.65
% Change	73.23	128.99	-40.01	0.14	-13.44	-36.17

Table 6. Post-hoc analysis of data examining rostral-caudal differences.
Increases in the GPi are large throughout, but more pronounced in caudal regions. Within the GPe, decreases appear to be solely within the rostral component. In the Pt, differences appear to be more caudal than rostral. (rGPi=rostral globus pallidus interna, cGPi=caudal globus pallidus interna; rGPe=rostral globus pallidus externa; cGPe=caudal globus pallidus externa; rPt=rostral putamen; cPt=caudal putamen)

III. Substance P and met-enkephalin staining

To assess whether functional neurotransmitter abnormalities may be present in TS, we performed immunostaining for substance P (SP) and met-enkephalin (enk), neuropeptides contained within striatal MSN of the direct and indirect pathways, respectively. Consistent with previous data,[68] SP-positive "woolly fibers" were concentrated in the GPi, suggesting that they represented terminals of the direct pathway; in contrast, enk-positive "woolly fibers" were greatly enriched in the GPe although a subset reached the GPi, consistent with being terminals of the indirect pathway. No qualitative difference in staining intensity within individual "woolly fibers" between cases and controls was apparent. A close comparison of sections for the TS and NC cases under examination showed no differences in the apparent density or distribution of fibers immunoreactive for these neuropeptides between NC and cases of TS (See Figure 7).

IV. Demographic data

No correlation was found between changes in PV or CV cell densities and neuroleptic intake or postmortem interval. While TS patients had co-morbid diagnoses, TS was the only diagnosis in common among them. Two patients had positive family histories of TS, and one had a perinatal hypoxic event; no obvious correlation existed between morphometric changes and suspected etiology. One control and one TS brain were at risk for secondary complications due to the agonal history (See Tables 1 and 2); however, no obvious correlations were found between this history and PV+ neuron number or density.

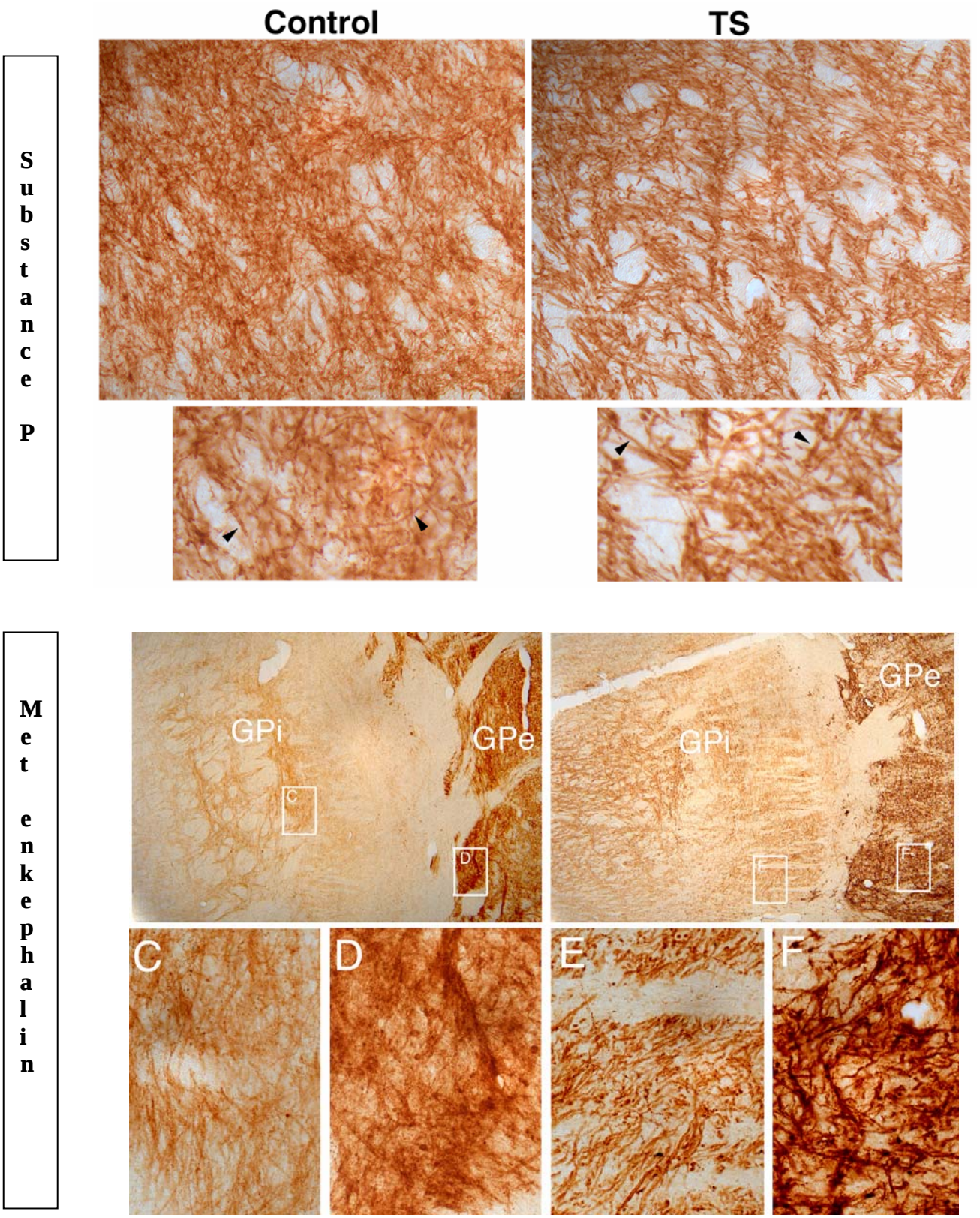

Figure 7. Met-enkephalin and Substance P Staining.

Staining for the MSN projections in the indirect (met-enkephalin) and direct (substance P) pathways revealed no apparent difference in morphology or density.

– DISCUSSION –

The data presented above provide the first quantitative cellular characterization of specific cell types within the basal ganglia of subjects with severe and persistent TS. Our data demonstrate a consistent and profound PV+ neuronal imbalance in the basal ganglia of the three patients examined. The striatum had fewer PV+ neurons, while the GPi had substantially more. These changes in the PV+ neuron distribution partially account for changes in the total neuron number in the GP subregions, which occurred in the absence of any change in volume or in glial cells. Using unbiased sampling methods, 54% and 35% decreases in PV neuron density were detected in the Cd and in Pt, respectively, of TS patients. The decrease in PV+ neurons in the Cd is consistent with the small (<5%) decreases in Cd volume which is present in both children and adults with TS,[69] a decrease that in children is also correlated with tic severity later in life.[5] Confirming earlier studies in TS,[70] no changes were detected in the apparent density of MSN projections in either the SP-immunoreactive direct or the enk-positive indirect pathways. However, we must await unbiased estimations of the total number of MSN using appropriate markers to definitively settle the question of whether MSN are altered in TS.

Taking the basal ganglia as a whole, there is a small (14%) non-significant decrease in PV+ neurons in TS (Table 5), while the distribution of PV cells is strikingly altered in TS, with far more PV+ cells in the GPi and substantially fewer in other regions of the BG, particularly the Cd. We think that it is unlikely that the above changes in PV+ neuron distribution are due to altered PV expression, for two reasons. First, the PV+

cell changes in the GPi are paralleled by changes in total neuron number, as assessed by cresyl violet staining; and second, it is improbable that variables that might affect the expression or the immunodetection of PV would manifest in opposite ways among basal ganglia subregions. For example, the increase in cresyl violet-stained neurons in the GPi from subjects with TS is fully accounted for by the increase in PV+ cells in this nucleus. Remarkably, both density and number of PV+ neurons were more than twice as large in TS as compared to NC. However, parvalbumin expression has been shown to be sensitive to neurotransmitter changes, such as those elicited by cocaine exposure,[71] and we cannot completely rule out that complex changes in both number of neurons and PV expression occur in TS.

Our data also suggest that other neuronal populations besides PV neurons may be affected in TS, because a 46.2% statistically significant decrease in total neuron number was observed in the GPe, whereas the density or number of PV+ cells is decreased on average by only 30% in this region (this decrease is not statistically significant, which may be a reflection of the small number of subjects). Similarly, our data may be interpreted to suggest a decrease in non-PV+ neurons in the GPi from subjects with TS, because the proportion of PV+ is much higher in the GPi of TS patients. These data suggest a possibility that parallel, opposite changes may be occurring in a PV-negative population of cells in the GPi in this disorder. The nature of these PV-negative neurons is currently under investigation. They appear to have a slightly different morphology as PV+ neurons[72] and location within the GPi[73] and some evidence suggests GP PV+ neurons primarily provide the BG output, as opposed to forming intra-BG connections.[74] While parvalbumin's calcium binding ability has been hypothesized to affect refractory hyperpolarization, and therefore, firing frequency,[75] whether there are

any functional differences between PV-positive and PV-negative neurons in the GP is currently unclear. Given that we did not specifically investigate PV-negative cells, further research examining these populations would have to be conducted to characterize these populations.

The data presented here have additional limitations. The small sample size may not be representative. However, the consistency of the results engendered statistical significance by non-parametric analysis.[‡] While TS is a neurodevelopmental disorder, our subjects, by necessity, were adults. This complicates the data in three ways. First, adult cases of TS may represent an atypical form of TS. Classical forms of TS may differ in the natural history and severity from adult TS. Classical TS usually peaks in adolescence with symptoms easing into adulthood, whereas adult TS persists and tends to be far more severe. Our subjects presented with extreme forms of TS, with almost maximum scores on TS rating scales. While studying extreme presentations of pathology has a long history of revealing mechanisms of more benign forms of disease, we cannot rule out that adult severe TS represents a separate disease with a distinct neural presentation. Second, the blocks of tissue available to us did not include certain portions of the basal ganglia circuit, including the SNr (which, however, may be a less important structure than the GPi in humans[25]) and STN. Moreover, we did not have access to other portions of the CTSC, including relevant areas of the cortex and thalamus. As such, we cannot rule out separate pathologies of these areas. However, while clinical and experimental data suggests that the thalamus and particularly areas of cortex may play an important role in TS, the BG, in particular the striatum, remain the

[‡] Further, additions of new TS brains analyzed by YK since the generation of the data discussed here have confirmed the initial results.

predominant area of interest. We only examined PV+ cell populations, but other interneuron populations may be affected as well.§ Additionally, while the statistically significant positive findings of the study suggest real differences, the small number of subjects precludes confidence in negative results. As such, other abnormalities in cell numbers may exist. Finally, our study shares the limitations of all neuropathologic studies. Based on purely immunohistochemical data, physiological conclusions cannot be firmly drawn. We cannot assert that our findings represent the original insult in TS nor can we rule out the possibility that our findings represent compensatory changes to a different pathology, or changes secondary to other phenomena, for example, medications taken. However, by attempting to locate our findings in the context of current and emerging understandings of basal ganglia function and dysfunction, the data are placed in their most likely context, and most importantly, testable hypotheses may be generated to confirm the theories of pathophysiology and etiology.

The PV+ neuron deficit in the TS striatum fits both traditional circuit-based models of basal ganglia pathophysiology[47, 76-79] as well as emerging oscillation models[49, 50]. In the traditional circuit, cortical input excites PV+ interneurons[80] which, in turn, powerfully inhibit MSNs[23], maintaining the characteristic low activity of the striatum. The loss of PV+ interneurons in this circuit would thus disinhibit MSNs, which should lead to MSN hyperactivity, GPi hypoactivity and increased thalamocortical firing, producing a hyperkinetic state.[79] Consistent with this hypothesis, as noted above, microstimulation of the Pt produces stereotypies, suggesting that local hyperactivity of MSNs can produce tics.

§ YK has performed an analysis of calretinin-positive cells, and initial data suggests that a subpopulation of them, likely identical to ACh interneurons, are decreased in density in TS in the Cd head by 64%.

The loss of PV+ interneurons leading to tics is also consistent with oscillatory models of BG function. Recent recordings from monkeys indicate that, when still, striatal activity is synchronized at a beta-band oscillatory frequency (15-30 Hz); during movement, certain localized striatal sites desynchronize, resynchronizing after the movement ceases.[81] PV activity may limit the spread and therefore the spatial extent of the striatal desychronization elicited by cortical inputs. Other in vivo recordings suggest that, at rest, high amplitude spindle and theta-band (~8 Hz) oscillatory frequencies are prominent in the striatum of awake rats.[20] Because PV+ striatal interneurons form an electrically coupled inhibitory network that can entrain very large assemblies of neurons,[19, 23, 24] the PV+ interneuron network may play a critical role in the synchrony of striatal oscillations and their modulation by the cerebral cortex and thalamus.[20] Hence a deficit in striatal PV+ interneurons may plausibly impair the PV+ interneuron network's ability to maintain synchrony, leading to inefficient production of oscillatory frequencies and inappropriate desynchrony of small populations of striatal MSN, resulting in tic-like behavior.

The potential role of PV+ interneuron deficits in promoting tic-like behavior finds confirmation in a hamster model of idiopathic paroxysmal dystonia. The *dt*^{sz} hamster phenotype shares many features with TS, including facial contortions, hyperextension of limbs, and co-contractions of opposing muscle groups[82] as well as a similar age-dependent time course.[83] Remarkably, the *dt*^{sz} hamster also has a lower striatal volume, and a strikingly similar reduction in striatal PV+ interneuron number (41% decrease,

compared to 53% decrease in TS).[84] These emerging lines of data strongly support a role for striatal PV+ interneuron deficit in TS and other hyperkinetic disorders.[**]

The contribution of the GPe to movement disorders is only recently emerging. Microinjection studies in monkeys provide evidence for the involvement of projections from the ventral Cd to the GPe in tic-like stereotypies.[86, 87] Connections between sensorimotor putamen, the GPe and the GPi appear to be involved in monkey models of dyskinesias,[87] and PV+ GPe cells may be specifically involved in the sensorimotor pathway.[88] The GPe receives projections from the striatal MSNs as part of the indirect pathway, and a reduction in cell number may represent a defect within this pathway, possibly allowing increased direct pathway activity, resulting in hyperkinesis. However, within the classic rate model of the BG, loss of GPe neural projections to the STN would result in disinhibition of the GPi, and thus, decreased thalamic activity, and thus, a hypokinetic state. As such, concordance with the rate model would require additional defects within the STN, or hyperactivity of the reduced number of GPe cells. Further, the GPe sends direct projections to all other nuclei of the basal ganglia, including projections to the striatum,[89] as well as the thalamus, and it appears to serve as a pacemaker of the basal ganglia.[90] Hence the overall 46% decrease in total neuron number in the GPe in our cohort of severe cases of TS may implicate a change in overall BG oscillatory activity.

Because the GPi is a major output of the basal ganglia and prominently involved in processing sensorimotor information, alterations of its structure are likely to figure

[**] It should be noted that, like our study, these studies did not assess other interneurons. Our emerging data suggests an additional decrease in a population of CR+ neurons, likely ACh neurons. Recent data shows a deficit in CR+ interneurons in this hamster model as well85.

Hamann M, Sander SE, Richter A. Age-dependent alterations of striatal calretinin interneuron density in a genetic animal model of primary paroxysmal dystonia. J Neuropathol Exp Neurol 2005; 64:776-81..

centrally in kinetic disorder pathophysiology. The striking changes in the GPi do not easily fit with rate models of the basal ganglia. An increase in GPi projection neurons, if all of them appropriately synapse within the thalamus, should inhibit thalamic activity, militating against hyperkinetic states. One possible explanation would be that these cells represent a compensatory mechanism in TS. However, such a theory has little support in the literature, relying on unknown mechanisms of significant neurogenesis. The presence of these cells with the rate model seems best explained by assuming they are dys- or non-functional, either a by-product of a compensatory or pathologic process.

Oscillatory models of BG function are more accommodating to alteration in GPi cell number. Recent models of basal ganglia function have suggested that altered patterns of GPi discharge might be important in movement disorders.[91] Recordings from the GPi analogue in the *dt*^{sz} hamster reveal stunningly aberrant firing patterns which decrease as the hamster ages and the symptoms disappear.[92] That the natural history of stereotypy within these hamsters and the natural history of the aberrant firing appear to mimic the natural history of TS is intriguing. Similarly irregular firing patterns have also been recorded in the GPi of humans either with severe dystonia or severe TS.[93] While it is possible that these firing patterns may be a downstream effect of striatal abnormalities in these conditions, they highlight the possible significance of an intrinsic GPi defect. Moreoever, some evidence suggests that placement of deep brain stimulation in the GPi, rather than the parafascicular or centromedian nuclei of the thalamus, may provide equal or superior control of tics.[35, 42, 43] An increase of over 100% of PV+ GPi neurons in TS may very well generate aberrant firing patterns, which in turn may elicit secondary effects at thalamic level. For example, excessive inhibitory input may provoke rebound

excitation in thalamic relay nuclei or alter the pace of their oscillatory activity.[94] Such phenomena might result in the premonitory sensory 'urges' so characteristic of TS.

The post-hoc analysis to more precisely localize neuronal abnormalities provides further grounds for future studies. Different CTSC pathways may also be differently susceptible to parvalbumin defects. While the sensorimotor channel appears to operate in the beta band of oscillations, the limbic pathway (assessed from recordings in the hippocampus and ventral striatum) appears to operate at a theta frequency.[20] A slower baseline frequency may be differentially sensitive to parvalbumin insults, or may reflect a lack of intrinsic PV+ activity. The rostral and caudal sections used to re-analyze the GP roughly constitute, respectively, the associative circuit from the sensorimotor circuit.[95] The Pt caudally is involved in the sensorimotor circuit, while the rostral Pt, together with the Cd, approximates the striatal portion of the associative circuit.[13] The GPi and Pt anomalies appear most severe within the sensorimotor areas, which fits well with the finding that poor performance on motor tasks in childhood predicts future tic severity.[6] Additionally, striatal PV+ interneurons receive both sensory and motor input from the cortex,[96] and may play a role in integrating this information; some of TS phenomena may be explained by a decoupling of sensory and motor input. The association areas of CTSC circuitry has defects in the striatum, GPi and perhaps also the GPe. The possibility that different CTSC circuits within the BG may be differently affected may help explain the phenotypic variety of TS, and perhaps wider neuropsychiatric disease. However, this data would have to be reproduced in a specific study to analyze different circuits within

the BG, which our study was not designed to do. Such data may further elucidate the neurobiology of TS.[††]

Because of the various important roles of the PV+ neurons in the basal ganglia, these major changes in PV+ neuron distribution can be expected to have a dramatic effect in CSTC functioning, and may suggest possible etiologies for TS. Increased investigation in interactions between dopamine and PV+ interneurons may be beneficial.[97] Given the variety of both severity and longevity of TS, TS may represent several different etiologies which result in variable parvalbumin-positive interneuron alterations. TS may have separate genetic or environmental causes, or may require varied combinations of each. The alterations demonstrated here, if related to TS etiology, would suggest problems in PV neuron development. Consistent with an altered distribution in the absence of major changes in number of PV cells would be a defect in PV+ cell migration, though problems in neurogenesis are possible as well.

PV+ interneurons tangentially migrate from the medial ganglionic eminence (MGE), the precursor of the GP, to the LGE, the precursor to the striatum, as well as to the cerebral cortex and hippocampus; in humans, this occurs between 24 weeks of gestational age through 1 month post-partum.[98] Embryonically, PV+ interneurons cells appear to preferentially receive cortical input, and are active during the formation of corticostriatal synapses, suggesting a role in appropriate striatal development[99]; thus, besides from the disruption in function directly from the altered distribution of these cells, striatal development may be additionally hampered.

[††] YK has done some preliminary work looking at anterior-posterior distinctions, confirming the rostral location of Pt PV+ deficiencies, and discovering that ACh interneurons may be preferentially depleted in the Cd head.

Environmental insults may not only damage PV+ cells during their perinatal migration. PV+ neurons appear susceptible to excitotoxic injury[100, 101] as well as being particularly vulnerable to ischemic insults.[102] Studies focusing on perinatal hypoxia, a known risk factor for TS, and PV+ striatal interneurons may be promising. Perinatal asphyxia in rats, for example, produces a substantial decrease in striatal PV+ interneurons as well as motor dyscoordination.[103]

Genetic causes may also play a role. The Nkx2.1 gene, which is necessary for the specification of the MGE, is also required for the specification of these interneurons of the striatum, while the Dlx1/Dlx2 genes are required for their migration.[104, 105] Thus, a possible explanation for our data is that abnormalities in these or related genes during development cause altered migration of neurons arising from the MGE in TS patients. It is interesting to note that haploinsufficiency for Nkx2.1 has been associated with a mild form of dyskinesia and chorea in humans.[106, 107]

The observations presented here demonstrate significant alterations in the PV neuron populations of the BG in TS. These findings appear to bolster current theories of TS pathophysiology and etiology, and, it is hoped, will open a new front of investigation in TS. These findings provide ammunition for hypothesis generation, which will need experimental testing. Development of a mouse model where PV+ neurons may be selectively lesioned would be of a great utility, and work on such a model is set to begin at Yale.

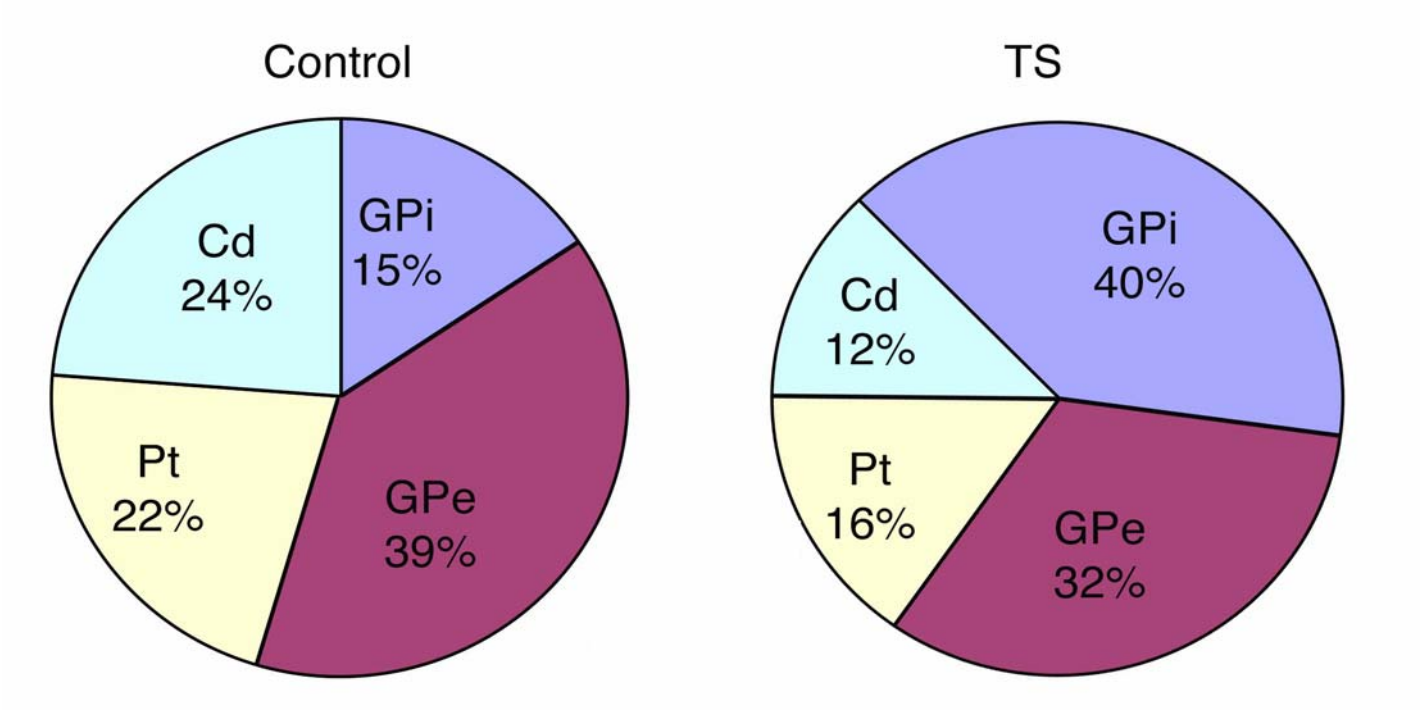

Figure 8. Distribution of PV+ cells throughout the striatum and globus pallidus. The location of PV+ cells differed between TS and control, with TS brains possessing a much larger proportion in the GPi, and far fewer in the striatum. No difference in total number was noted, though small sample size could explain this.

Figure 9. The migratory path of parvalbumin-positive cells.

During development, parvalbumin-positive cells originate in the medial ganglionic eminence (MGE), which itself develops into the globus pallidus. Cells migrate from the MGE to the lateral ganglionic eminence (LGE). The LGE develops into the striatum. The distribution of parvalbumin-positive cells described above is thus consistent with a defect in migration of this cell population.

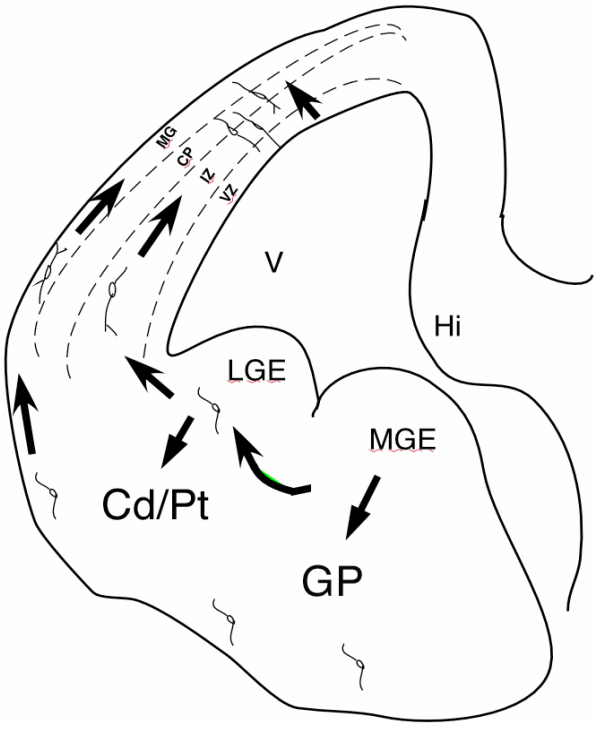

Ultimately, our data serves both to highlight an important circuit in TS pathology as well as an underutilized research methodology in neuropsychiatric diseases. Our research suggests the importance of the ACh-PV-MSN striatal circuit, as well as directing further research towards the GPi. The importance of clarifying the neural circuitry of TS remains important not only for understanding it and related diseases, but for developing treatments. In severe cases of TS, deep brain stimulation electrodes are positioned to affect the circuitry discussed here; clarifying the activity of this circuitry may help optimize treatment. Moreover, our work demonstrates the fruitfulness of quantitative immunohistochemistry in investigating neuropsychiatric disease. Since the publication of our data[64] and an accompanying paper on PV+ cells and oscillatory frequencies,[50] other studies have been produced highlighting the importance of gamma oscillations and deficiencies of other PV+ networks in other neuropsychiatric diseases.[108, 109] Defects in PV+ interneuron networks may play a significant role in explaining neuropsychiatric disease. The contributions of our work, we hope, are three-fold: a robust defense of stereologic techniques in exploring neuropsychiatric disease; the first quantitative pathological demonstration of a neural defect in TS; and the first discovery of the link between the PV+ interneuron network and human neuropsychiatric disease.

– References –

1. Hornsey H, Banerjee, S., Zeitlin, H., Robertson, M. The prevalence of Tourette syndrome in 13–14-year-olds in mainstream schools. J Child Psychol Psychiatry 2001; 42:1035–1039.
2. Leckman JF, Zhang H, Vitale A, et al. Course of tic severity in Tourette syndrome: the first two decades. Pediatrics 1998; 102:14-9.
3. Bloch MH, Peterson BS, Scahill L, et al. Adulthood outcome of tic and obsessive-compulsive symptom severity in children with Tourette syndrome. Arch Pediatr Adolesc Med 2006; 160:65-9.
4. Erenberg G, Cruse RP, Rothner AD. The natural history of Tourette syndrome: a follow-up study. Ann Neurol 1987; 22:383-5.
5. Bloch MH, Leckman JF, Zhu H, Peterson BS. Caudate volumes in childhood predict symptom severity in adults with Tourette syndrome. Neurology 2005; 65:1253-8.
6. Bloch MH, Sukhodolsky DG, Leckman JF, Schultz RT. Fine-motor skill deficits in childhood predict adulthood tic severity and global psychosocial functioning in Tourette's syndrome. J Child Psychol Psychiatry 2006; 47:551-9.
7. Leckman JF, Bloch MH, Scahill L, King RA. Tourette syndrome: the self under siege. J Child Neurol 2006; 21:642-9.
8. Leckman JF, Riddle MA, Hardin MT, et al. The Yale Global Tic Severity Scale: initial testing of a clinician-rated scale of tic severity. J Am Acad Child Adolesc Psychiatry 1989; 28:566-73.
9. Sheppard DM, Bradshaw JL, Purcell R, Pantelis C. Tourette's and comorbid syndromes: obsessive compulsive and attention deficit hyperactivity disorder. A common etiology? Clin Psychol Rev 1999; 19:531-52.
10. Abelson JF, Kwan KY, O'Roak BJ, et al. Sequence variants in SLITRK1 are associated with Tourette's syndrome. Science 2005; 310:317-20.
11. Leckman JF. Tourette's syndrome. Lancet 2002; 360:1577-86.
12. Whitaker AH, Van Rossem R, Feldman JF, et al. Psychiatric outcome in low-birth-weight children at age 6 years: relation to neonatal cranial ultrasound abnormalities. Arch Gen Psychiatry 1997; 54:847-856.
13. Parent A, Hazrati LN. Functional anatomy of the basal ganglia. I. The cortico-basal ganglia-thalamo-cortical loop. Brain Res Brain Res Rev 1995; 20:91-127.
14. Alexander GE, DeLong MR, Strick PL. Parallel organization of functionally segregated circuits linking basal ganglia and cortex. Annu Rev Neurosci 1986; 9:357-81.
15. Holt DJ, Graybiel AM, Saper CB. Neurochemical architecture of the human striatum. J Comp Neurol 1997; 384:1-25.
16. Kimura M, Yamada H, Matsumoto N. Tonically active neurons in the striatum encode motivational contexts of action. Brain Dev 2003; 25 Suppl 1:S20-3.
17. Koos T, Tepper JM. Dual cholinergic control of fast-spiking interneurons in the neostriatum. J Neurosci 2002; 22:529-35.
18. Wilson CJ. Postsynaptic potentials evoked in spiny neostriatal projection neurons by stimulation of ipsilateral and contralateral neocortex. Brain Res 1986; 367:201-13.
19. Kita H, Kosaka T, Heizmann CW. Parvalbumin-immunoreactive neurons in the rat neostriatum: a light and electron microscopy study. Brain Res. 1990; 536:1-15.

20. Berke JD, Okatan M, Skurski J, Eichenbaum HB. Oscillatory entrainment of striatal neurons in freely moving rats. Neuron 2004; 43:883-96.
21. Koos T, Tepper JM, Wilson CJ. Comparison of IPSCs evoked by spiny and fast-spiking neurons in the neostriatum. J Neurosci 2004; 24:7916-22.
22. Tepper JM, Koos T, Wilson CJ. GABAergic microcircuits in the neostriatum. Trends Neurosci 2004; 27:662-9.
23. Koos T, Tepper JM. Inhibitory control of neostriatal projection neurons by GABAergic interneurons. Nat Neurosci 1999; 2:467-72.
24. Plenz D. When inhibition goes incognito: feedback interaction between spiny projection neurons in striatal function. Trends Neurosci 2003; 26:436-43.
25. Hardman CD, Henderson JM, Finkelstein DI, Horne MK, Paxinos G, Halliday GM. Comparison of the basal ganglia in rats, marmosets, macaques, baboons, and humans: volume and neuronal number for the output, internal relay, and striatal modulating nuclei. J Comp Neurol 2002; 445:238-55.
26. Hardman CD, Halliday GM. The external globus pallidus in patients with Parkinson's disease and progressive supranuclear palsy. Movement Disorders 1999; 14:626-33.
27. Albin RL, Young AB, Penney JB. The functional anatomy of basal ganglia disorders. TINS 1989; 12:366-375.
28. Alexander GE, DeLong MR. Microstimulation of the primate neostriatum. II. Somatotopic organization of striatal microexcitable zones and their relation to neuronal response properties. J Neurophysiol 1985; 53:1417-30.
29. Peterson BS, Thomas P, Kane MJ, et al. Basal Ganglia volumes in patients with Gilles de la Tourette syndrome. Arch Gen Psychiatry 2003; 60:415-24.
30. Stoetter B, Braun AR, Randolph C, et al. Functional neuroanatomy of Tourette syndrome. Limbic-motor interactions studied with FDG PET. Adv Neurol 1992; 58:213-26.
31. Braun AR, Stoetter B, Randolph C, et al. The functional neuroanatomy of Tourette's syndrome: an FDG-PET study. I. Regional changes in cerebral glucose metabolism differentiating patients and controls. Neuropsychopharmacology 1993; 9:277-91.
32. Chase TN, Geoffrey V, Gillespie M, Burrows GH. Structural and functional studies of Gilles de la Tourette syndrome. Rev Neurol (Paris) 1986; 142:851-5.
33. Albin RL, Koeppe RA, Bohnen NI, et al. Increased ventral striatal monoaminergic innervation in Tourette syndrome. Neurology 2003; 61:310-5.
34. Peterson BS, Skudlarski P, Anderson AW, et al. A functional magnetic resonance imaging study of tic suppression in Tourette syndrome. Arch Gen Psychiatry 1998; 55:326-33.
35. Shahed J, Poysky J, Kenney C, Simpson R, Jankovic J. GPi deep brain stimulation for Tourette syndrome improves tics and psychiatric comorbidities. Neurology 2007; 68:159-60.
36. Halpern C, Hurtig H, Jaggi J, Grossman M, Won M, Baltuch G. Deep brain stimulation in neurologic disorders. Parkinsonism Relat Disord 2007; 13:1-16.
37. Hardesty DE, Sackeim HA. Deep Brain Stimulation in Movement and Psychiatric Disorders. Biol Psychiatry 2006.
38. Mink JW, Walkup J, Frey KA, et al. Patient selection and assessment recommendations for deep brain stimulation in Tourette syndrome. Mov Disord 2006; 21:1831-8.

39. Neimat JS, Patil PG, Lozano AM. Novel surgical therapies for Tourette syndrome. J Child Neurol 2006; 21:715-8.
40. Malone DA, Jr., Pandya MM. Behavioral neurosurgery. Adv Neurol 2006; 99:241-7.
41. Visser-Vandewalle V, Ackermans L, van der Linden C, et al. Deep brain stimulation in Gilles de la Tourette's syndrome. Neurosurgery 2006; 58:E590.
42. Ackermans L, Temel Y, Cath D, et al. Deep brain stimulation in Tourette's syndrome: two targets? Mov Disord 2006; 21:709-13.
43. Diederich NJ, Kalteis K, Stamenkovic M, Pieri V, Alesch F. Efficient internal pallidal stimulation in Gilles de la Tourette syndrome: a case report. Mov Disord 2005; 20:1496-9.
44. Houeto JL, Karachi C, Mallet L, et al. Tourette's syndrome and deep brain stimulation. J Neurol Neurosurg Psychiatry 2005; 76:992-5.
45. Visser-Vandewalle V, Temel Y, van der Linden C, Ackermans L, Beuls E. Deep brain stimulation in movement disorders. The applications reconsidered. Acta Neurol Belg 2004; 104:33-6.
46. Temel Y, Visser-Vandewalle V. Surgery in Tourette syndrome. Mov Disord 2004; 19:3-14.
47. Mink JW. The Basal Ganglia and involuntary movements: impaired inhibition of competing motor patterns. Arch Neurol 2003; 60:1365-8.
48. Cunningham MO, Whittington MA, Bibbig A, et al. A role for fast rhythmic bursting neurons in cortical gamma oscillations in vitro. Proc Natl Acad Sci U S A 2004; 101:7152-7.
49. Hutchison WD, Dostrovsky JO, Walters JR, et al. Neuronal oscillations in the basal ganglia and movement disorders: evidence from whole animal and human recordings. J Neurosci 2004; 24:9240-3.
50. Leckman JF, Vaccarino FM, Kalanithi PS, Rothenberger A. Annotation: Tourette syndrome: a relentless drumbeat--driven by misguided brain oscillations. J Child Psychol Psychiatry 2006; 47:537-50.
51. Nambu A, Llinas R. Electrophysiology of globus pallidus neurons in vitro. J Neurophysiol 1994; 72:1127-39.
52. Steriade M, Timofeev I. Neuronal plasticity in thalamocortical networks during sleep and waking oscillations. Neuron 2003; 37:563-76.
53. Adams P, Cox K. A new interpretation of thalamocortical circuitry. Philos Trans R Soc Lond B Biol Sci 2002; 357:1767-79.
54. Kawaguchi Y. Physiological, morphological, and histochemical characterization of three classes of interneurons in rat neostriatum. J Neurosci 1993; 13:4908-23.
55. Kubota Y, Mikawa S, Kawaguchi Y. Neostriatal GABAergic interneurones contain NOS, calretinin or parvalbumin. Neuroreport 1993; 5:205-8.
56. Mallet N, Le Moine C, Charpier S, Gonon F. Feedforward inhibition of projection neurons by fast-spiking GABA interneurons in the rat striatum in vivo. J Neurosci 2005; 25:3857-69.
57. Galarreta M, Hestrin S. Spike transmission and synchrony detection in networks of GABAergic interneurons. Science 2001; 292:2295-9.
58. Mallet N, Ballion B, Le Moine C, Gonon F. Cortical inputs and GABA interneurons imbalance projection neurons in the striatum of parkinsonian rats. J Neurosci 2006; 26:3875-84.

59. Galarreta M, Hestrin S. A network of fast-spiking cells in the neocortex connected by electrical synapses. Nature 1999; 402:72-5.
60. Galarreta M, Hestrin S. Electrical synapses between GABA-releasing interneurons. Nat Rev Neurosci 2001; 2:425-33.
61. Galarreta M, Hestrin S. Electrical and chemical synapses among parvalbumin fast-spiking GABAergic interneurons in adult mouse neocortex. Proc Natl Acad Sci U S A 2002; 99:12438-43.
62. Leckman JF, Sholomskas D, Thompson WD, Belanger A, Weissman MM. Best estimate of lifetime psychiatric diagnosis: a methodological study. Arch Gen Psychiatry 1982; 39:879-83.
63. Robertson MM, Banerjee S, Kurlan R, et al. The Tourette syndrome diagnostic confidence index: development and clinical associations. Neurology 1999; 53:2108-12.
64. Kalanithi PS, Zheng W, Kataoka Y, et al. Altered parvalbumin-positive neuron distribution in basal ganglia of individuals with Tourette syndrome. Proc Natl Acad Sci U S A 2005; 102:13307-12.
65. Gundersen HJ, Bagger P, Bendtsen TF, et al. The new stereological tools: disector, fractionator, nucleator, and point sampled intercepts and their use in pathological research and diagnosis. APMIS 1988; 96:857-881.
66. West MJ. New Stereological Methods for Counting Neurons. Neurobiology of Aging 1993; 14:275-285.
67. Morel A, Loup F, Magnin M, Jeanmonod D. Neurochemical organization of the human basal ganglia: anatomofunctional territories defined by the distributions of calcium-binding proteins and SMI-32. J Comp Neurol 2002; 443:86-103.
68. Haber SN, Watson SJ. The comparative distribution of enkephalin, dynorphin and substance P in the human globus pallidus and basal forebrain. Neuroscience 1985; 14:1011-24.
69. Peterson B, Riddle MA, Cohen DJ, et al. Reduced basal ganglia volumes in Tourette's syndrome using three-dimensional reconstruction techniques from magnetic resonance images. Neurology 1993; 43:941-9.
70. Haber SN, Kowall NW, Vonsattel JP, Bird ED, Richardson EP, Jr. Gilles de la Tourette's syndrome. A postmortem neuropathological and immunohistochemical study. J Neurol Sci 1986; 75:225-41.
71. Todtenkopf MS, Stellar JR, Williams EA, Zahm DS. Differential distribution of parvalbumin immunoreactive neurons in the striatum of cocaine sensitized rats. Neuroscience 2004; 127:35-42.
72. Kita H. Parvalbumin-immunopositive neurons in rat globus pallidus: a light and electron microscopic study. Brain Res 1994; 657:31-41.
73. Hontanilla B, Parent A, Gimenez-Amaya JM. Compartmental distribution of parvalbumin and calbindin D-28k in rat globus pallidus. Neuroreport 1994; 5:2269-72.
74. Shammah-Lagnado SJ, Alheid GF, Heimer L. Efferent connections of the caudal part of the globus pallidus in the rat. J Comp Neurol 1996; 376:489-507.
75. Celio MR. Calbindin D-28k and parvalbumin in the rat nervous system. Neuroscience 1990; 35:375-475.
76. Singer HS, Minzer K. Neurobiology of Tourette's syndrome: concepts of neuroanatomic localization and neurochemical abnormalities. Brain Dev 2003; 25 Suppl 1:S70-84.

77. Mink JW. Neurobiology of basal ganglia circuits in Tourette syndrome: faulty inhibition of unwanted motor patterns? Adv Neurol 2001; 85:113-22.
78. Mink JW. Basal ganglia dysfunction in Tourette's syndrome: a new hypothesis. Pediatr Neurol 2001; 25:190-8.
79. Mink JW. Neurobiology of basal ganglia and Tourette syndrome: basal ganglia circuits and thalamocortical outputs. Adv Neurol 2006; 99:89-98.
80. Kita H. GABAergic circuits of the striatum. Prog Brain Res 1993; 99:51-72.
81. Courtemanche R, Fujii N, Graybiel AM. Synchronous, focally modulated beta-band oscillations characterize local field potential activity in the striatum of awake behaving monkeys. J Neurosci 2003; 23:11741-52.
82. Loscher W, Fisher JE, Jr., Schmidt D, Fredow G, Honack D, Iturrian WB. The sz mutant hamster: a genetic model of epilepsy or of paroxysmal dystonia? Mov Disord 1989; 4:219-32.
83. Richter A, Loscher W. Pathology of idiopathic dystonia: findings from genetic animal models. Prog Neurobiol 1998; 54:633-77.
84. Gernert M, Hamann M, Bennay M, Loscher W, Richter A. Deficit of striatal parvalbumin-reactive GABAergic interneurons and decreased basal ganglia output in a genetic rodent model of idiopathic paroxysmal dystonia. J Neurosci 2000; 20:7052-8.
85. Hamann M, Sander SE, Richter A. Age-dependent alterations of striatal calretinin interneuron density in a genetic animal model of primary paroxysmal dystonia. J Neuropathol Exp Neurol 2005; 64:776-81.
86. Grabli D, McCairn K, Hirsch EC, et al. Behavioural disorders induced by external globus pallidus dysfunction in primates: I. Behavioural study. Brain 2004; 127:2039-54.
87. Francois C, Grabli D, McCairn K, et al. Behavioural disorders induced by external globus pallidus dysfunction in primates II. Anatomical study. Brain 2004; 127:2055-70.
88. Rajakumar N, Rushlow W, Naus CC, Elisevich K, Flumerfelt BA. Neurochemical compartmentalization of the globus pallidus in the rat: an immunocytochemical study of calcium-binding proteins. J Comp Neurol 1994; 346:337-48.
89. Kita H, Tokuno H, Nambu A. Monkey globus pallidus external segment neurons projecting to the neostriatum. Neuroreport 1999; 10:1467-72.
90. Plenz D, Kital ST. A basal ganglia pacemaker formed by the subthalamic nucleus and external globus pallidus. Nature 1999; 400:677-82.
91. Wichmann T, DeLong MR. Functional and pathophysiological models of the basal ganglia. Curr Opin Neurobiol 1996; 6:751-8.
92. Gernert M, Bennay M, Fedrowitz M, Rehders JH, Richter A. Altered discharge pattern of basal ganglia output neurons in an animal model of idiopathic dystonia. J Neurosci 2002; 22:7244-53.
93. Zhuang P, Li Y, Hallett M. Neuronal activity in the basal ganglia and thalamus in patients with dystonia. Clin Neurophysiol 2004; 115:2542-57.
94. Pedroarena C, Llinas R. Dendritic calcium conductances generate high-frequency oscillation in thalamocortical neurons. Proc Natl Acad Sci U S A 1997; 94:724-8.
95. Parent A, Cicchetti F, Beach TG. Calretinin-immunoreactive neurons in the human striatum. Brain Res 1995; 674:347-51.
96. Ramanathan S, Hanley JJ, Deniau JM, Bolam JP. Synaptic convergence of motor and somatosensory cortical afferents onto GABAergic interneurons in the rat striatum. J Neurosci 2002; 22:8158-69.

97. Trevitt JT, Morrow J, Marshall JF. Dopamine manipulation alters immediate-early gene response of striatal parvalbumin interneurons to cortical stimulation. Brain Res 2005; 1035:41-50.
98. Iai M, Takashima S. Thalamocortical development of parvalbumin neurons in normal and periventricular leukomalacia brains. Neuropediatrics 1999; 30:14-8.
99. Plotkin JL, Wu N, Chesselet MF, Levine MS. Functional and molecular development of striatal fast-spiking GABAergic interneurons and their cortical inputs. Eur J Neurosci 2005; 22:1097-108.
100. Pezzi S, Checa N, Alberch J. The vulnerability of striatal projection neurons and interneurons to excitotoxicity is differentially regulated by dopamine during development. Int J Dev Neurosci 2005; 23:343-9.
101. Maetzler W, Nitsch C, Bendfeldt K, Racay P, Vollenweider F, Schwaller B. Ectopic parvalbumin expression in mouse forebrain neurons increases excitotoxic injury provoked by ibotenic acid injection into the striatum. Exp Neurol 2004; 186:78-88.
102. Larsson E, Lindvall O, Kokaia Z. Stereological assessment of vulnerability of immunocytochemically identified striatal and hippocampal neurons after global cerebral ischemia in rats. Brain Res 2001; 913:117-32.
103. Van de Berg WD, Kwaijtaal M, de Louw AJ, et al. Impact of perinatal asphyxia on the GABAergic and locomotor system. Neuroscience 2003; 117:83-96.
104. Anderson SA, Marin O, Horn C, Jennings K, Rubenstein JL. Distinct cortical migrations from the medial and lateral ganglionic eminences. Development 2001; 128:353-363.
105. Anderson S, Mione M, Yun K, Rubenstein JLR. Differential origins of neocortical projectionn and local circuit neurons: role of Dlx genes in neocortical interneurogenesis. Cereb.Cortex 1999; 9:647-654.
106. Pohlenz J, Dumitrescu A, Zundel D, et al. Partial deficiency of thyroid transcription factor 1 produces predominantly neurological defects in humans and mice. J Clin Invest 2002; 109:469-73.
107. Breedveld GJ, van Dongen JW, Danesino C, et al. Mutations in TITF-1 are associated with benign hereditary chorea. Hum Mol Genet 2002; 11:971-9.
108. Cunningham MO, Hunt, J., Middleton, S., LeBeau, F., Gillies, M., Davies, C., Maycox, P., Whittington, M., Racca, C. Region-Specific Reduction in Entorhinal Gamma Oscillations and Parvalbumin-Immunoreactive Neurons in Animal Models of Psychiatric Illness. Journal of Neuroscience 2006; 26:2767-2776.
109. Rajkowska G, O'Dwyer G, Teleki Z, Stockmeier CA, Miguel-Hidalgo JJ. GABAergic neurons immunoreactive for calcium binding proteins are reduced in the prefrontal cortex in major depression. Neuropsychopharmacology 2007; 32:471-82.